

Van der Waals Complexes of Small Molecules with Benzenoid Rings: Influence of Multipole Moments on Their Mutual Orientation

Brijesh Kumar Mishra and N. Sathyamurthy*

Department of Chemistry, Indian Institute of Technology Kanpur, Kanpur 208016, India

Received: August 29, 2006; In Final Form: January 15, 2007

Intermolecular interaction between some small molecules (HF, H₂O, NH₃, and CH₄) and certain benzenoid ring systems (benzene, hexafluorobenzene, and 1,3,5-trifluorobenzene) has been investigated in detail at MP2 level of theory using 6-311++G** basis set, and the results are corrected for basis set superposition error (BSSE). Vibrational frequencies were calculated for all the geometries at the same level of theory and basis sets to ensure that the geometries obtained correspond to true minima. In the complexes with benzene, which has a large negative quadrupole moment, the preferred geometry has the electropositive end of the small molecule (HF, H₂O, and NH₃) pointing toward the ring and the corresponding interaction energies are −3.24, −2.43, and −1.57 kcal/mol, respectively. For the complexes with hexafluorobenzene which has a large positive quadrupole moment, the most stable geometries are those in which the electropositive end of HF, H₂O, and NH₃ points away from the ring and the corresponding interaction energies are −1.59, −2.73, and −3.14 kcal/mol, respectively. Methane, which has neither a dipole nor a quadrupole moment, is weakly bound and is oriented differently in different systems. 1,3,5-Trifluorobenzene has a negligible quadrupole moment, and the complexes with small molecules are stabilized by cyclic hydrogen bonding. Although the point dipole–quadrupole and point quadrupole–quadrupole interactions present in these complexes account qualitatively for the preferred orientations, distributed multipole moments of the constituent atoms are found to give a quantitative description of the interaction in such complexes.

1. Introduction

Van der Waals (vdW) forces are responsible for most of the chemical and physical properties of matter. They play an important role in supramolecular chemistry, in molecular crystal packing, in solvation phenomena, in the structures of biomacromolecules such as DNA and proteins, and in molecular recognition processes. As compared to covalent bonds, which have a binding energy ~100 kcal/mol, van der Waals interaction and hydrogen bond are in the range 0.1–10 kcal/mol. vdW interaction can generally be accounted for in terms of permanent, induced, and instantaneous multipole moments of the molecules involved.

Some of the early theoretical developments toward understanding the vdW interaction were reviewed by Margenau in 1939.¹ Interaction between central multipole moments of two molecules was systematically formulated by Buckingham² and later reformulated by Stone.³ Structures of various vdW complexes were analyzed by Fowler and Buckingham using a model on the basis of electrostatic interaction and hard-sphere repulsion.⁴ For the molecular adduct between a sym-triazine and 1,3,5-trifluorobenzene, Fowler and Buckingham⁵ showed that the central multipole model failed to describe the electrostatic interaction and was divergent. Therefore, they proposed a distributed point-multipole model.

Major advances in both theoretical and experimental methods for studying van der Waals complexes in the last two decades have been reviewed extensively.^{6–9} The benzene–water complex has been a system of extensive investigation.^{10–16} Rota-

tionally resolved spectrum of C₆H₆–H₂O complex revealed that both the hydrogen atoms of the water molecule point toward the benzene ring.¹⁰ The interaction energy was computed to be −1.78 kcal/mol at second-order Møller–Plesset perturbation (MP2) level of theory. Subsequently, the rotational spectra of C₆H₆–H₂O¹¹ and C₆H₆–H₂S complexes¹² were recorded by Gutowsky and co-workers. Barth et al. reported the first experimental investigation of hydrogen bonding in substituted benzene–(H₂O)_n clusters.¹³ Spectroscopic measurements for C₆H₆–NH₃ complex were reported by Rodham et al.,¹⁷ and it was shown that ammonia molecule was positioned on the top of benzene ring with the hydrogen atoms pointing toward the ring.

Using MP2 level of theory, quantum mechanical probabilistic structure of the C₆H₆–H₂O complex was studied,¹⁸ and two geometries, “leg one” in which one hydrogen atom of the H₂O molecule points toward the center of the benzene ring and “leg two” in which both the hydrogen atoms point toward the ring, were found to be nearly isoenergetic. Feller¹⁹ showed that the geometry in which one of the hydrogen atoms of the water molecule points toward the benzene ring is the most stable and the interaction energy was computed as −3.9 ± 0.2 kcal/mol at the MP2 level of theory using a very large basis set. Ab initio calculations at the MP2 level of theory using 6-311++G** basis set were performed by Tarakeshwar et al.²⁰ for C₆H₆–HF and C₆H₆–HCl complexes. For C₆H₆–HF, the interaction energies (uncorrected) for three geometries (on-atom, on-bond, and C_{6v}) were −5.56, −5.56, and −5.53 kcal/mol, respectively. Tsuzuki et al.²¹ examined the intermolecular interaction in C₆H₆–H₂O, C₆H₆–NH₃, and C₆H₆–CH₄ complexes at the MP2 level, in the extrapolated basis set limit and also applying a correction

* To whom correspondence should be addressed. E-mail: nsath@iitk.ac.in.

using coupled cluster calculations with single and double excitations including noniterative triples (CCSD(T)). The interaction energy was found to be -3.17 , -2.22 , and -1.45 kcal/mol, respectively. The interaction energy of C_6H_6 with chloro- and fluoromethanes²² increased with increased substitution of the hydrogen atoms in methane. The interaction between pyridine and small molecules (H_2O , NH_3 , and CH_4) was investigated at MP2 level of theory for a large number of geometries (with 50% basis set superposition error (BSSE) correction) by Samanta et al.²³ Intermolecular interaction between C_6H_6 and some hydrocarbon molecules (methane, ethane, ethylene, and acetylene) was carried out by Tsuzuki et al.²⁴ using the MP2 method at the basis set limit and CCSD(T) correction terms.

The effect of perfluorination of benzene on the orientation of small molecules has been reported by several researchers.^{25–32} Molecular beam studies of vdW complexes of C_6H_6 , C_6F_6 , and sym- $C_6H_3F_3$ with HF by Baiocchi et al.³³ indicated that the fluorine-substituted benzene ring forms a π complex less easily than benzene. Theoretical calculations for fluorobenzene– H_2O and *p*-difluorobenzene– H_2O systems by Tarakeshwar et al.³⁴ at the MP2 level of theory using various basis sets showed that the most stable geometry involved in-plane hydrogen bonds. The O–H part of the water molecule forms hydrogen bonds with the fluorine atom and the nearest neighboring hydrogen atom of the aromatic ring resulting in a six-membered cyclic ring. The microwave spectrum for fluorobenzene–HCl complex was recorded by Sanz et al.,³⁵ and it was concluded that HCl lay above the fluorobenzene ring near the ring center, similar to the C_6H_6 –HCl complex. Ab initio calculations (MP2/6-311++G(2df,2pd)+CP(BSSE)) revealed that the π complex is more stable than the σ complex (in-plane hydrogen-bonded geometry). C_6H_6 – C_6F_6 complex was studied and the role of molecular quadrupole moment in deciding the mutual orientation between molecules was discussed by Williams.³⁶ Calculations on C_6F_6 – H_2O complex³⁷ revealed that the most stable geometry has the oxygen atom of the H_2O molecule facing the ring. The interaction energy for the complex benzene–water–hexafluorobenzene trimer was computed by Raimondi et al.³⁸ The water molecule was sandwiched in the complex such that hydrogen atom of water molecule faces the benzene ring and oxygen atom points toward hexafluorobenzene ring.

The stacking interaction in C_6H_6 dimer in different orientations was studied³⁹ using CCSD(T) method, and the calculated interaction energies for parallel, T-shaped, and slipped-parallel geometries were -1.48 , -2.46 , and -2.48 kcal/mol, respectively. This stability order can be accounted for in terms of quadrupole–quadrupole interaction. Interaction in substituted benzene dimers (C_6H_6 –phenol, C_6H_6 –toluene, C_6H_6 –fluorobenzene, and C_6H_6 –benzonitrile) was investigated by Sinokrot and Sherrill,⁴⁰ and the results showed that the substituted sandwich dimers bind more strongly than benzene dimer. The π – π interaction in pyridine dimer and trimer for different geometries at the MP2 level of theory using different basis sets was investigated by us.⁴¹ The antiparallel-displaced geometry in which the dipole moments were oriented in opposite directions was the most stable. Pyrazine molecule has zero dipole moment but a nonzero quadrupole moment. Therefore, it is expected that the mutual orientation of the pyrazine monomers in the dimer would be dictated by quadrupole–quadrupole interaction. CCSD(T) calculations⁴² showed the pyrazine dimer to be the most stable in a T-shaped geometry, akin to that of benzene dimer.

Benzene, hexafluorobenzene, and 1,3,5-trifluorobenzene serve as prototypes of three distinct classes of molecules in terms of their electric quadrupole moment. While benzene has a large negative quadrupole moment, hexafluorobenzene has a large positive quadrupole moment and 1,3,5-trifluorobenzene has negligible quadrupole moment. Therefore, a systematic ab initio investigation of the interaction between small molecules and the above-mentioned benzenoid ring systems was undertaken, and the results were interpreted in terms of multipole interactions. The basic methodology used is described in section 2. Results and discussion follow in section 3. Summary and conclusion are given in section 4.

2. Methodology

Gaussian 03 suite of programs⁴³ was used for the electronic structure calculations. Geometry optimization and frequency calculation for all the complexes under investigation were carried out at the MP2 level of theory using 6-311++G** basis set. The interaction energy (ΔE) was computed using the supermolecule approach:

$$\Delta E = E_{AB}^{\alpha\cup\beta}(AB) - E_A^\alpha(A) - E_B^\beta(B) \quad (1)$$

where the energy E of a molecule M in geometry G computed with basis set σ is represented as $E_G^\sigma(M)$.

The results were corrected for basis set superposition error (BSSE) using the counterpoise correction method,⁴⁴ and the corrected interaction energies were calculated using the equation

$$\Delta E(\text{BSSE}) = E_{AB}^{\alpha\cup\beta}(AB) - E_{AB}^{\alpha\cup\beta}(A) - E_{AB}^{\alpha\cup\beta}(B) + E_{\text{rel}}^\alpha(A) + E_{\text{rel}}^\beta(B) \quad (2)$$

where

$$E_{\text{rel}}^\alpha(A) = E_{AB}^\alpha(A) - E_A^\alpha(A), \quad E_{\text{rel}}^\beta(B) = E_{AB}^\beta(B) - E_B^\beta(B) \quad (3)$$

The molecular dipole and quadrupole moments were calculated using the same level of theory and the basis set. Quadrupole moment is a tensor of rank two. Therefore, in Cartesian coordinates, there will be six (xx , xy , xz , yy , yz , zz) independent terms. Since the molecules under investigation are axisymmetrical, only diagonal terms (xx , yy , zz) would survive. Interestingly, only one component (zz) is found to be independent for all the molecules except H_2O and one can relate the three components of quadrupole moment using a simple equation:

$$Q_{xx} = Q_{yy} = -\frac{Q_{zz}}{2} \quad (4)$$

For H_2O , Q_{zz} is the smallest. In the point multipole model, the dipole–quadrupole interaction is calculated as follows:

$$\Delta E = \pm 3 \times \frac{|M_{zz}^A| \times Q_{zz}^B}{R^4} \quad (5)$$

the “+” sign being applicable when the dipole moment of molecule A points toward the aromatic ring B and the “–” sign being applicable when the dipole moment of A points away from the ring of B . When the small molecule A lies on top of the ring B along the z -axis (perpendicular to the ring, passing through the center of mass of the ring), the quadrupole–quadrupole interaction is calculated as follows:

$$\Delta E = 6 \times \frac{Q_{zz}^A \times Q_{zz}^B}{R^5} \quad (6)$$

Distributed multipoles of rank up to four were computed from the MP2/6-311G** wave functions for all atoms in the individual molecules of the vdW complexes using CADPAC version 6.⁴⁵ Electrostatic interaction arising from these distributed multipole moments was calculated using the software package Orient, version 3.2.⁴⁶ The dispersion and repulsion energies between the molecules were also calculated with the help of Orient program,⁴⁶ which uses an exp-6 atom-atom potential:

$$U_{\text{exp-6}} = \sum_{a \in A} \sum_{b \in B} K \exp(-\alpha_{ab}(R_{ab} - \rho_{ab})) - \frac{C_6^{ab}}{R_{ab}^6} \quad (7)$$

where a and b represent atom sites and the sum is over all the atoms in each molecule. The parameters α , ρ , and C_6 for all atom pairs were taken from ref 3. The pre-exponential factor K is chosen such that the energy is in millihartree units.

3. Results and Discussion

3.1. Energy and Stability of Various Geometries. The fully optimized geometries of C_6H_6-X , C_6F_6-X , and $C_6H_3F_3-X$ complexes, where $X = HF$, H_2O , NH_3 , and CH_4 , are illustrated in Figure 1, Figure 2, and Figure 3, respectively. Frequency calculations have been carried out for each energetically stable geometry. The number of imaginary frequencies corresponding to a particular complex is mentioned in all the figures in the top right corner. The other details pertaining to the frequency analysis are given in the Supporting Information. The interaction energies for all the complexes are listed in Table 1. The value of R listed therein refers to the distance between the heavy atom in molecule X and the center of mass of the benzenoid moiety. The electrostatic (ΔE_{es}), dispersion (ΔE_{dis}), and repulsion (ΔE_{rep}) energies are reported in Table 2. The calculated values of electric dipole and electric quadrupole moments are listed and compared with experimental results⁴⁷ in Table 3. Table 4 contains dipole-dipole and dipole-quadrupole interactions for top-on complexes. The geometry of the individual molecules in the complex is almost the same as in the free state. Hence, the details are not reported in this paper.

For C_6H_6-HF complex, there are four different optimized geometries shown in Figure 1. The most stable geometry corresponds to 1a(iv) ($\Delta E = -3.24$ kcal/mol) in which HF is oriented perpendicular to the plane of the benzene ring (H atom pointing toward the ring) with an offset of 0.47 Å from the center of the ring (C_s point group). Despite the energy of 1a(i) being comparable to that of 1a(iv), the frequency calculation reveals two imaginary frequencies for the former, indicative of a saddle point on the potential energy surface. Interestingly, the most stable geometry 1a(iv) does not correspond to C_{6v} symmetry as predicted by Brèdas and Street.⁴⁸ Geometry shown in Figure 1a(ii) is energetically unstable and the hydrogen-bonded complex 1a(iii) has three imaginary frequencies.

In $C_6H_6-H_2O$ complex, “leg1” (1b(i)) and “leg2” (1b(ii)) geometries are found to be nearly isoenergetic, with an interaction energy of -2.43 and -2.48 kcal/mol, respectively. It is seen from the frequency calculation that the geometry 1b(i) is a true minimum but the geometry 1b(ii) is a saddle. The geometry 1b(iii) in which the O atom of H_2O points toward the benzene ring is unstable. The end-on planar geometry 1b(iv) is only weakly bound ($\Delta E = -0.98$ kcal/mol) and has three

imaginary frequencies. In the most stable geometry leg1, one of the O-H bonds of water molecule is pointing parallel to one of the C-H bonds of the ring.

For $C_6H_6-NH_3$, leg1 geometry (1c(i)) ($\Delta E = -1.57$ kcal/mol) is slightly more stable than leg3 (1c(ii)) ($\Delta E = -1.31$ kcal/mol). Similar to the $C_6H_6-H_2O$ complex, here too the frequency calculations identify leg1 geometry to be the true minimum and the leg3 geometry to be a saddle. When the ammonia molecule is inverted, that is, the N atom points toward the ring, the complex 1c(iii) becomes unstable. The interaction energy for the weakly hydrogen-bonded geometry 1c(iv) is $\Delta E = -1.26$ kcal/mol with two imaginary frequencies.

In the case of $C_6H_6-CH_4$ complex, even though the stabilization energies for leg1 (Figure 1d(i); $\Delta E = -0.85$ kcal/mol) and leg3 (Figure 1d(ii); $\Delta E = -0.94$ kcal/mol) geometries are comparable, the frequency calculation identifies the leg1 geometry to be the true minimum and the latter has two imaginary frequencies.

In summary, when the hydrogen atom of the participating molecule X points toward the benzene ring (leg1 geometry where applicable), the complex is a true minimum and the complex becomes unstable when the electronegative atom points toward the C_6H_6 ring. Contrary to the intuitive expectations, most symmetric geometries for the respective complexes were found not to be stable. There does not exist any stable geometry in the close proximity of leg2 and leg3 geometries for the corresponding complexes. This was verified by performing geometry search in which force constants were computed at every stage and all leg2 and leg3 geometries led to leg1 geometry.

The orientation of the small molecules with respect to hexafluorobenzene is opposite to that for benzene. In the most stable geometry of C_6F_6-HF (2a(i)), HF is perpendicular to the ring with the F atom pointing toward the center of the ring (C_{6v} point group) with interaction energy $\Delta E = -1.59$ kcal/mol. This is nearly half of what was reported for the most stable geometry for C_6H_6-HF . The geometry 2a(ii) is unstable, in contrast to that of the corresponding C_6H_6-HF complex. The interaction energy of the end-on hydrogen-bonded (F...H-F) complex is found to be -1.56 kcal/mol, but the frequency calculation revealed it to be a saddle.

In the case of the vdW complex with H_2O , the most stable geometry 2b(ii) has the O atom pointing toward the ring placed at a distance of 2.95 Å, with an offset from the center being 0.21 Å (interaction energy $\Delta E = -2.73$ kcal/mol). The geometry shown in 2b(i) though being symmetric and shown to be a minimum²⁷ is in fact a saddle with two imaginary frequencies. Contrary to the complex with benzene, the leg2 (2b(iii)) geometry is unstable. Two end-on planar geometries, one with one hydrogen bond (2b(iv), $\Delta E = -0.60$ kcal/mol) and the other with two hydrogen bonds (2b(iv), $\Delta E = -0.87$ kcal/mol), are found to be saddle points.

Similar to H_2O , the “N” atom of NH_3 prefers to face the center of the benzenoid ring as shown in Figure 2c(i), with an interaction energy $\Delta E = -3.14$ kcal/mol. No stable end-on hydrogen-bonded geometry is found for $C_6F_6-NH_3$. Geometry optimization starting from an end-on geometry results in 2c(ii), similar to 2c(i), but with a slight shift and an inclination of NH_3 molecule with respect to the ring ($\Delta E = -2.94$ kcal/mol). Surprisingly, the leg3 (2c(iii)) geometry is weakly bound with the stabilization energy -0.36 kcal/mol.

In $C_6F_6-CH_4$, leg1 (2d(i)), leg3 (2d(ii)), and end-on 2d(iii) geometries are found to have stabilization energies $\Delta E = -0.94$, -1.25 , and -0.50 kcal/mol, respectively, with all of them having

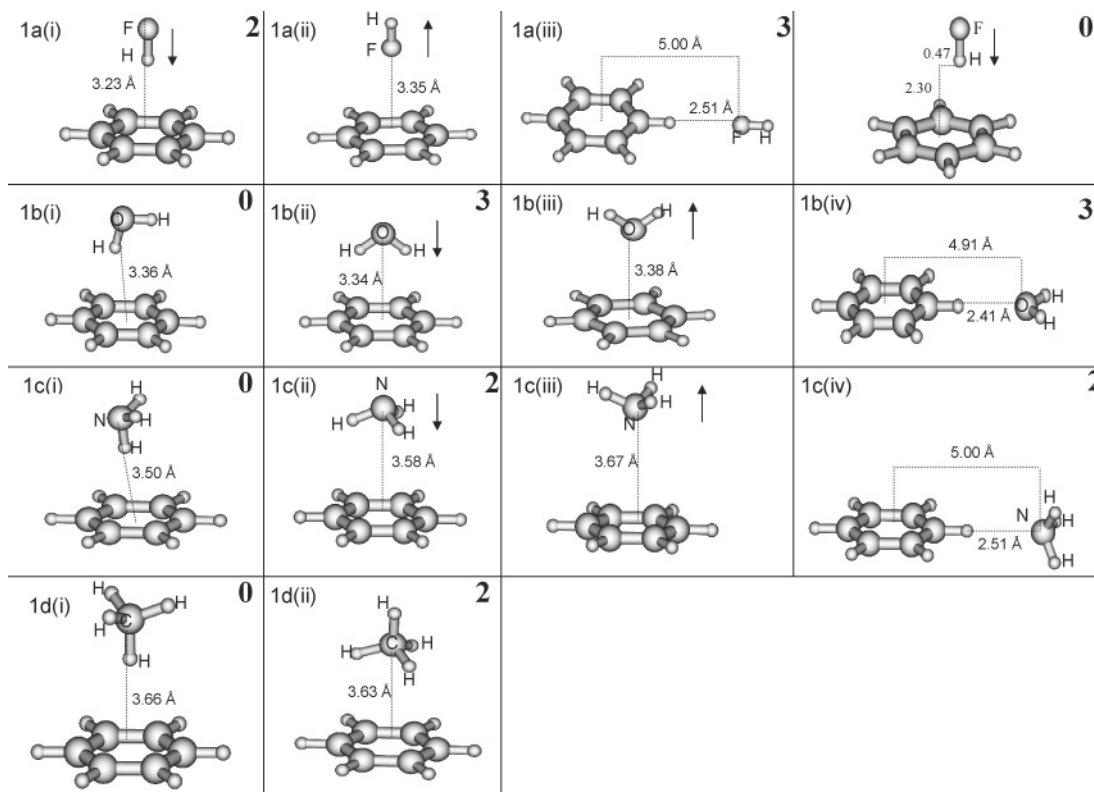


Figure 1. Fully optimized geometries at MP2/6-311++G** level of theory for C_6H_6-X complexes, where $X = HF, H_2O, NH_3,$ and CH_4 in different orientations. The numbers in bold letters in the corner of each panel for an “energetically stable” complex indicate the number of imaginary frequencies.

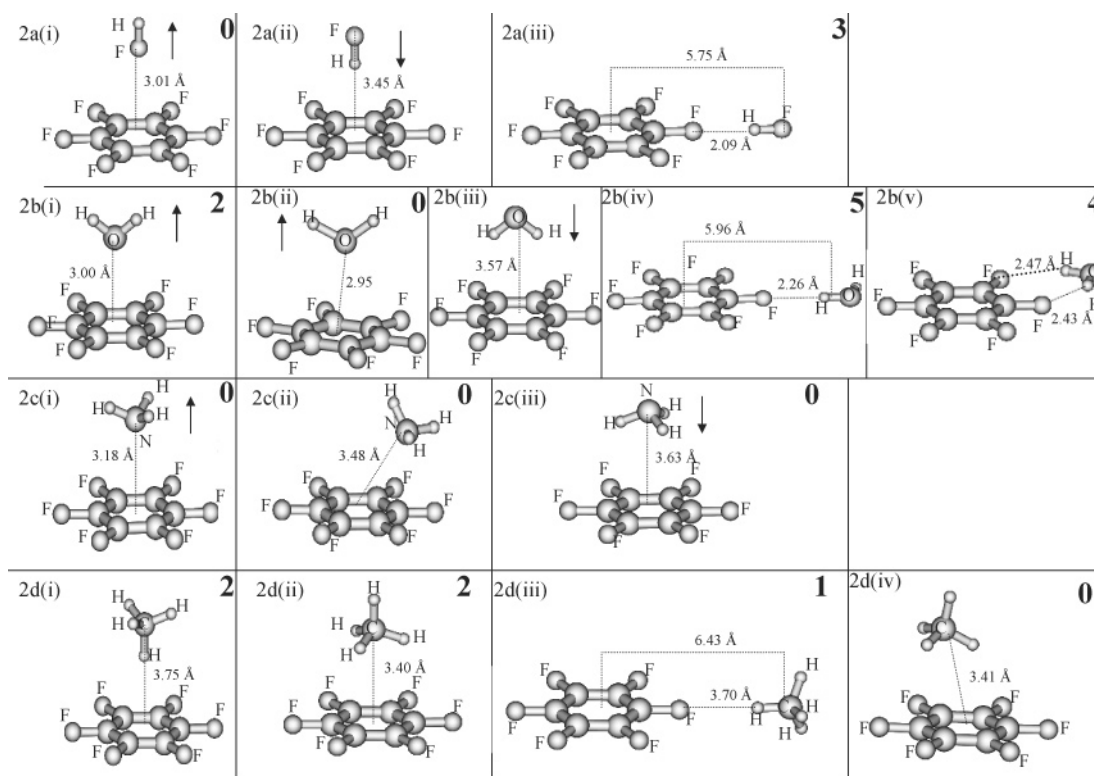


Figure 2. Same as in Figure 1 for C_6F_6-X complexes.

imaginary frequencies. Furthermore, an extensive search for a true minimum for the methane complex resulted in a top-on geometry (2d(iv)) which is moderately stable ($\Delta E = -1.15$ kcal/mol). The methane molecule lies on the top of a carbon atom of the ring and one of the H atoms of methane points toward the center of the ring.

In summary, it is seen that in C_6F_6 the F atom does not participate in hydrogen bonding. The small molecule orients itself in such a fashion that the more electronegative atom points toward the ring.

Contrary to C_6H_6-HF and C_6F_6-HF complexes, the $C_6H_3F_3-HF$ complex is least stable when HF is perpendicular to the

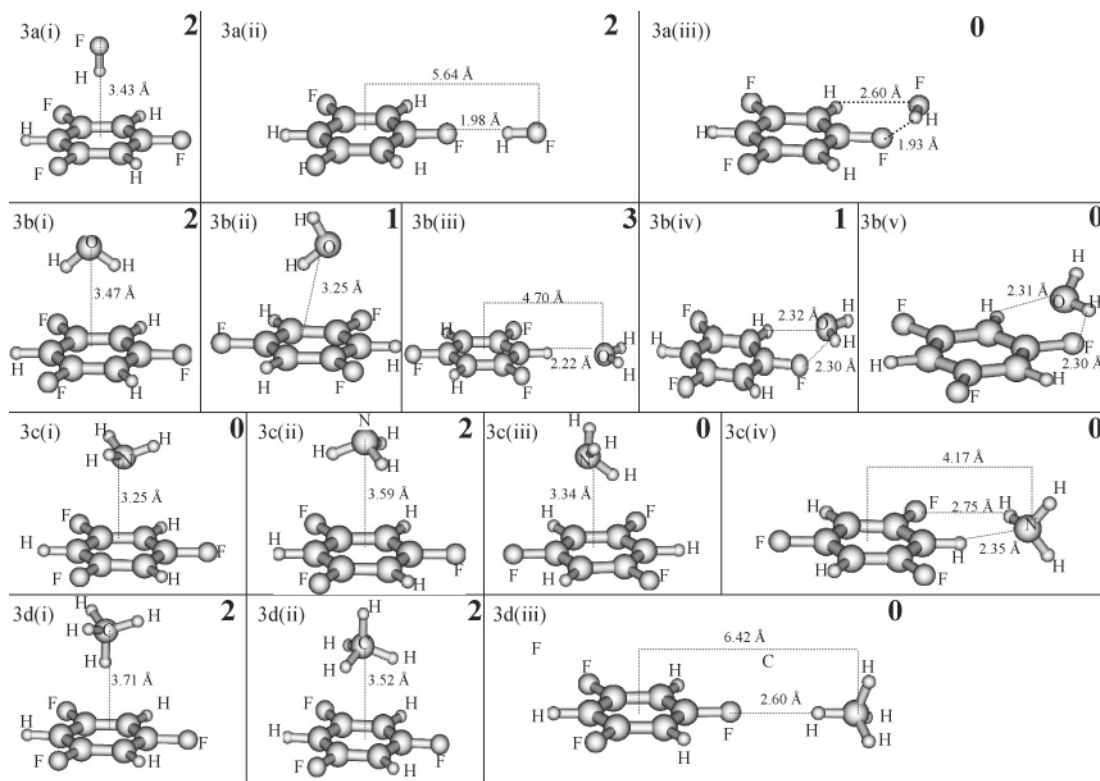


Figure 3. Same as in Figure 1 for $C_6H_3F_3-X$ complexes.

ring (Figure 3a(i)) with $\Delta E = -0.78$ kcal/mol). HF prefers to form hydrogen bonds with one of the F atoms of $C_6H_3F_3$, as illustrated in Figure 3a(ii) and 3a(iii), with $\Delta E = -2.62$ kcal/mol and -2.71 kcal/mol, respectively. The frequency calculations show 3a(iii) to be a true minimum. The formation of a six-membered ring as a consequence of the hydrogen bond formation can be attributed as a cause for this stability of 3a(iii).

Extensive search for a stable geometry in the case of $C_6H_3F_3-H_2O$ complex resulted in those shown in Figure 3a(i–v). Energetically, the hydrogen-bonded geometries (3b(iii), 3b(iv), and 3b(v)) are more stable than the remaining ones. However, among the hydrogen-bonded ones, the frequency calculation distinctly identifies 3b(v) to be the most stable ($\Delta E = -2.86$ kcal/mol). 3b(iv) is almost similar with respect to the geometry as well as the energy. However, the former is a saddle. The formation of a six-membered ring as a consequence of two hydrogen bonds of type $F...H-O$ and $C-H...O$ becomes evident in Figure 3b(v), with one of the hydrogen atoms of the water molecule remaining out of the plane of the ring.

Four optimized geometries are shown for $C_6H_3F_3-NH_3$ complex in Figure 3c(i–iv). Geometries 3c(i) and 3c(iii) have comparable stabilization energies ($\Delta E = -0.87$ and -0.97 kcal/mol, respectively), and the most stable geometry, 3c(iv), has -2.87 kcal/mol as its stabilization energy. Here again, the formation of a cyclic hydrogen-bonded complex contributes to the stability. Frequency calculations identify 3c(ii) to be a saddle.

Three plausible geometries were optimized in the case of $C_6H_3F_3-CH_4$ complex, among which 3d(iii), a hydrogen-bonded complex ($F...H-C$), is seen to be a stable geometry ($\Delta E = -0.20$ kcal/mol). The stabilization energy of trifluorobenzene (with a negligible quadrupole moment) complex with methane (with zero quadrupole moment) is expectedly very low. Calculations reveal that the other geometries are in fact not true minima. In 3d(iii), one of the hydrogen atoms of methane makes a

dihedral angle very close to 90° with respect to the plane of the ring (details (side view) are shown in Supporting Information).

3.2. Interaction between Point Multipole Moments. Some of the trends observed in the most stable geometries for the C_6H_6-X , C_6F_6-X , and $C_6H_3F_3-X$ complexes can be understood in terms of dipole–quadrupole (D–Q) and quadrupole–quadrupole (Q–Q) interactions. While benzene has a large negative quadrupole moment (-8.38 debye \AA), hexafluorobenzene has a large positive quadrupole moment (9.24 debye \AA) and 1,3,5-trifluorobenzene has negligible quadrupole moment (0.84 debye \AA). Since the zz component of the quadrupole moment is the largest, only the top-on geometries have been considered. The values of ΔE_{D-Q} and ΔE_{Q-Q} listed in Table 4 show clearly that the D–Q interaction changes sign as geometries of small molecules are inverted. Since CH_4 has neither dipole nor quadrupole moment, the electrostatic contribution for stability is zero. Benzene and hexafluorobenzene have comparable quadrupole moments, although different in sign. Therefore, their interaction energies with $X = HF, H_2O,$ and NH_3 are comparable. Since $C_6H_3F_3$ has a quadrupole moment close to zero, its electrostatic interaction for top-on geometries is the least. Under the point multipole approximation, D–Q and Q–Q interactions are highly sensitive to the center-of-mass separation (R).

3.3. The Role of Electrostatic, Repulsion, and Dispersion Energies. For a more detailed understanding of the trends in the computed ab initio results for the different vdW complexes, an energy decomposition analysis was performed. The electrostatic interaction arising from distributed multipole moments, Pauli repulsion and London dispersion energies as obtained from eq 7, are listed in Table 2.

For C_6H_6-HF , the geometries 1a(i) and 1a(iv) have a large positive repulsion energy ($\Delta E_{rep} = 3.04, 3.51$ kcal/mol, respectively) outweighing the attractive dispersion energy ($\Delta E_{dis} =$

TABLE 1: Interaction Energies (kcal/mol) for C_6H_6-X , C_6F_6-X , and $C_6H_3F_3-X$ Complexes, Where $X = HF, H_2O, NH_3$, and CH_4 in Different Orientations Obtained at MP2 Level of Theory Using 6-311++G Basis Set**

	$R(\text{\AA}), r(\text{\AA})$	ΔE_{MP2}	ΔE_{MP2} (BSSE corrected)
C_6H_6-HF			
1a(i)	3.23	-5.42	-3.15
1a(ii)	3.35	-0.14	0.91
1a(iii)	5.00	-1.03	-0.57
1a(iv)	2.30, 0.47	-5.44	-3.24
$C_6H_6-H_2O$			
1b(i)	3.36	-4.51	-2.43
1b(ii)	3.34	-4.30	-2.48
1b(iii)	3.38	-0.17	1.11
1b(iv)	4.91	-1.96	-0.98
$C_6H_6-NH_3$			
1c(i)	3.50	-3.52	-1.57
1c(ii)	3.58	-2.89	-1.31
1c(iii)	3.67	-0.31	0.92
1c(iv)	5.00	-2.57	-1.26
$C_6H_6-CH_4$			
1d(i)	3.66	-2.66	-0.85
1d(ii)	3.63	-2.25	-0.94
C_6F_6-HF			
2a(i)	3.01	-3.35	-1.59
2a(ii)	3.45	-0.58	1.34
2a(iii)	5.75	-2.00	-1.56
$C_6F_6-H_2O$			
2b(i)	3.00	-4.77	-2.67
2b(ii)	2.95	-4.98	-2.73
2b(iii)	3.57	-1.28	+0.76
2b(iv)	5.96	-1.39	-0.60
2b(v)	5.34	-1.96	-0.87
$C_6F_6-NH_3$			
2c(i)	3.18	-5.46	-3.14
2c(ii)	3.48	-5.40	-2.94
2c(iii)	3.63	-2.30	-0.36
$C_6F_6-CH_4$			
2d(i)	3.75	-2.93	-0.94
2d(ii)	3.40	-3.37	-1.25
2d(iii)	6.43	-0.90	-0.50
2d(iv)	3.41	-3.49	-1.15
$C_6H_3F_3-HF$			
3a(i)	3.43	-2.55	-0.78
3a(ii)	5.64	-3.06	-2.62
3a(iii)	4.62	-4.04	-2.71
$C_6H_3F_3-H_2O$			
3b(i)	3.47	-2.65	-0.72
3b(ii)	3.25	-2.73	-0.83
3b(iii)	4.70	-3.68	-2.36
3b(iv)	4.53	-4.16	-2.93
3b(v)	2.31, 2.30	-4.37	-2.86
$C_6H_3F_3-NH_3$			
3c(i)	3.25	-2.72	-0.87
3c(ii)	3.59	-2.42	-0.58
3c(iii)	3.34	-2.89	-0.97
3c(iv)	4.17	-4.44	-2.87
$C_6H_3F_3-CH_4$			
4d(i)	3.71	-2.50	-0.79
4d(ii)	3.52	-2.64	-0.90
4d(iii)	6.42	-0.72	-0.21

-2.81, -2.91 kcal/mol, respectively), and major stabilization comes from the electrostatic attraction ($\Delta E_{es} = -3.77, -3.98$ kcal/mol, respectively). On the other hand, for the geometry 1a(ii), both repulsion and dispersion energies are relatively small in magnitude and the electrostatic interaction is repulsive, resulting in destabilization of the complex. For the end-on hydrogen-bonded geometry 1a(iii), the individual components

TABLE 2: Electrostatic (ΔE_{es}), Repulsion (ΔE_{rep}), and Dispersion (ΔE_{dis}) Energies (kcal/mol) for the C_6H_6-X , C_6F_6-X , and $C_6H_3F_3-X$ Complexes, Where $X = HF, H_2O, NH_3$, and CH_4 for Different Orientations Using MP2/6-311G Wave Functions**

	ΔE_{es}	ΔE_{rep}	ΔE_{dis}	ΔE_{total}
C_6H_6-HF				
1a(i)	-3.77	3.04	-2.81	-3.54
1a(ii)	1.67	0.24	-0.83	1.08
1a(iii)	-0.51	0.14	-0.36	-0.73
1a(iv)	-3.98	3.51	-2.91	-3.38
$C_6H_6-H_2O$				
1b(i)	-2.50	1.31	-2.23	-3.42
1b(ii)	-2.83	1.68	-2.78	-3.93
1b(iii)	2.50	0.29	-1.21	1.58
1b(iv)	-1.26	0.82	-0.94	-1.37
$C_6H_6-NH_3$				
1c(i)	-1.41	1.91	-2.58	-2.08
1c(ii)	-0.98	0.66	-2.02	-2.34
1c(iii)	2.44	0.19	-1.03	1.60
1c(iv)	-1.90	0.76	-0.92	-2.06
$C_6H_6-CH_4$				
1d(i)	-0.26	1.34	-2.34	-1.26
1d(ii)	0.23	0.62	-2.05	-1.20
C_6F_6-HF				
2a(i)	-1.84	0.94	-1.59	-2.49
2a(ii)	3.26	1.47	-2.07	2.66
2a(iii)	-0.97	0.63	-0.67	-1.01
$C_6F_6-H_2O$				
2b(i)	-2.75	1.21	-2.38	-3.92
2b(ii)	-2.73	1.91	-2.35	-3.89
2b(iii)	1.95	0.71	-2.05	0.61
2b(iv)	-0.67	1.15	-0.93	-0.45
2b(v)	-1.08	1.19	-1.47	-1.36
$C_6F_6-NH_3$				
2c(i)	-3.12	1.06	-2.29	-4.35
2c(ii)	-3.06	1.31	-2.19	-3.94
2c(iii)	0.65	0.56	-2.04	-0.83
$C_6F_6-CH_4$				
2d(i)	0.19	1.20	-2.40	-1.01
2d(ii)	-0.20	1.08	-2.79	-1.91
2d(iii)	0.01	0.28	-0.53	-0.24
2d(iv)	-0.07	1.36	-2.99	-1.74
$C_6H_3F_3-HF$				
3a(i)	0.24	1.57	-2.03	-0.22
3a(ii)	-1.52	0.94	-0.76	-1.34
3a(iii)	-3.87	5.52	-2.58	-0.93
$C_6H_3F_3-H_2O$				
3b(i)	-0.16	1.09	-2.36	-1.43
3b(ii)	-0.04	1.60	-2.58	-1.02
3b(iii)	-3.20	1.81	-1.45	-2.84
3b(iv)	-3.77	2.71	-2.31	-3.37
3b(v)	-3.83	2.75	-2.33	-3.37
$C_6H_3F_3-NH_3$				
3c(i)	-0.09	0.68	-1.82	-1.23
3c(ii)	-0.09	0.58	-1.99	-1.50
3c(iii)	-0.06	1.36	-2.42	-1.12
3c(iv)	-4.26	1.77	-1.75	-4.24
$C_6H_3F_3-CH_4$				
3d(i)	0.02	1.17	-2.30	-1.11
3d(ii)	0.03	0.83	-2.41	-1.55
3d(iii)	-0.04	0.28	-0.51	-0.27

(ΔE_{dis} , ΔE_{rep} , and ΔE_{es}) are not significant when compared to the values for other geometries.

Similarly, the 1b(i) and 1b(ii) geometries for $C_6H_6-H_2O$ and 1c(i) and 1c(ii) geometries for $C_6H_6-NH_3$ are stabilized by both electrostatic and dispersion energies. In contrast, the geometries 1b(iii) and 1c(iii) in which the electronegative atom points toward the benzene ring are unstable because of nonattractive

TABLE 3: Molecular Dipole and Quadrupole Moments at MP2 Level of Theory Using 6-311++G Basis Set**

	dipole moment (μ) in debye		quadrupole moment (Q) in debye Å in Cartesian frame	
	theoretical	expt	theoretical	expt
HF	1.97	1.91 ^a	$Q_{xx} = -1.04$ $Q_{yy} = -1.04$ $Q_{zz} = +2.08$	$Q_{zz} = +2.53^b$
water	2.19	1.85 ^a	$Q_{xx} = -2.33$ $Q_{yy} = +2.66$ $Q_{zz} = -0.33$	$Q_{xx} = -2.50^b$ $Q_{yy} = +2.64^b$ $Q_{zz} = -0.13^b$
ammonia	1.73	1.47 ^a	$Q_{xx} = 1.70$ $Q_{yy} = 1.70$ $Q_{zz} = -3.40$	
methane	0.00	0.00 ^a	$Q_{xx} = 0.00$ $Q_{yy} = 0.00$ $Q_{zz} = 0.00$	$Q_{zz} = 0.00$
benzene	0.00	0.00 ^a	$Q_{xx} = 4.19$ $Q_{yy} = 4.19$ $Q_{zz} = -8.38$	$Q_{zz} = -8.67^c$
hexafluorobenzene	0.00	0.00 ^a	$Q_{xx} = -4.62$ $Q_{yy} = -4.62$ $Q_{zz} = 9.24$	$Q_{zz} = 9.50^c$
1,3,5,-trifluorobenzene	0.00	0.00 ^a	$Q_{xx} = -0.42$ $Q_{yy} = -0.42$ $Q_{zz} = +0.84$	$Q_{zz} = +0.93^c$

^a Reference 47. ^b Reference 3. ^c Reference 36.

TABLE 4: Dipole–Quadrupole (ΔE_{D-Q}) and Quadrupole–Quadrupole (ΔE_{Q-Q}) Interaction Energies (kcal/mol) for Top-On Geometries

	ΔE_{D-Q}	ΔE_{Q-Q}	$\Delta E_{D-Q} + \Delta E_{Q-Q}$
		C₆H₆–HF	
1a(i)	–6.52	–4.30	–10.82
1a(ii)	5.67	–3.58	2.09
		C₆H₆–H₂O	
1b(ii)	–6.55	0.59	–5.96
1b(iii)	6.23	0.56	6.79
		C₆H₆–NH₃	
1c(ii)	–3.82	4.20	0.38
1c(iii)	3.46	3.71	7.17
		C₆H₆–CH₄	
1d(i)	0.00	0.00	0.00
1d(ii)	0.00	0.00	0.00
		C₆F₆–HF	
2a(i)	–6.05	3.99	–2.26
2a(ii)	5.35	3.40	8.95
		C₆F₆–H₂O	
2b(i)	–11.01	–1.11	–12.12
2b(iii)	5.48	–0.46	5.02
		C₆H₆–NH₃	
2c(i)	–6.89	–8.56	–15.45
2c(iii)	4.06	–4.41	–0.35
		C₆H₃F₃–HF	
3a(i)	–0.86	0.61	–0.25

electrostatic interaction. In the case of end-on geometry (1b (iv) and 1c(iv)) in which H₂O and NH₃ form weak hydrogen bonds, the stabilization is partly attributed to the electrostatic interaction. In C₆H₆–CH₄ complexes, for both geometries (leg1 and leg3), the electrostatic interaction contribution is insignificant and the complexes are stabilized by dispersion energy.

For the most stable geometry of C₆F₆–HF (2a(i)), ΔE_{es} (–1.84 kcal/mol) is attractive. However, for geometry 2a(ii), ΔE_{es} (+3.26 kcal/mol) is highly repulsive in nature. The hydrogen-bonded geometry 2a(iii) is also weakly stabilized by electrostatic interaction (–0.97 kcal/mol).

In C₆F₆–H₂O, both the geometries 2b(i) (C_{2v}) and 2b(ii) are almost similar in energy with a marginal difference in the energy components. Both are stabilized by dispersion energy ($\Delta E_{dis} = -2.38$ and -2.35 kcal/mol) and electrostatic energy ($\Delta E_{es} = -2.75$ and -2.73 kcal/mol). In the case of 2b(iii) where the geometry of water is inverted, the electrostatic interaction is repulsive in nature ($\Delta E_{es} = 1.95$ kcal/mol). ΔE_{es} is also accountable for both hydrogen-bonded geometries (2b(iv) and 2b(v)) but to a lesser extent. None of the hydrogen-bonded complexes are stable as stated earlier in the text.

In C₆F₆–NH₃ complex, 2c(i) and 2c(ii) geometries in which the nitrogen atom points toward the ring are stabilized by both dispersion ($\Delta E_{dis} = -2.29$ and -2.19 kcal/mol) and electrostatic energy ($\Delta E_{es} = -3.12$ and -3.06 kcal/mol). The electrostatic energy is repulsive for leg3 (2c(iii)) geometry, but the complex is stabilized by dispersion energy. Yet, it is weakly bound compared to the 2c(i) and 2c(ii) geometries.

For C₆F₆–CH₄, the geometry (2d(iv)) is the most stable as stated above with the stabilization energy -1.74 kcal/mol. In this complex, dispersion energy is maximum, when compared to the other complexes. The electrostatic energy is insignificant for all the geometries.

For C₆H₃F₃–HF, ΔE_{es} is insignificant for the geometry 3a-(i) (0.24 kcal/mol). The effect of attractive ΔE_{dis} is diminished by positive ΔE_{rep} . However, hydrogen-bonded geometries 3a-(ii) and 3a(iii) are stabilized by both ΔE_{dis} (–0.76 and -2.58 kcal/mol, respectively) and ΔE_{es} (–1.52 kcal/mol and -3.87 kcal/mol, respectively). Similarly for C₆F₃H₃–H₂O, ΔE_{es} for geometries 3b(i) and 3b(ii) are -0.16 and -0.04 , respectively, which are clearly not significant. The hydrogen-bonded geometries 3b(iii), 3b(iv), and 3b(v), are stabilized by both ΔE_{es} and ΔE_{dis} . In the case of the complex with NH₃, ΔE_{es} is negligible for the top-on geometries 3c(i), 3c(ii), and 3c(iii). The dispersion energy is the only source of attraction for these three geometries. For 3c(iv), ΔE_{es} , ΔE_{rep} , and ΔE_{dis} are -4.26 , 1.77 , and -1.75 kcal/mol, respectively. For all the geometries of C₆F₃H₃–CH₄, ΔE_{es} is extremely small and the complex is stabilized only by the dispersion energy.

3.4. Molecular Electrostatic Potential Maps. The role of the electrostatic potential for atoms, molecules, and weakly bonded complexes has been discussed by Gadre and co-workers.^{49–51} The electrostatic potential maps shown in Figures 4 and 5 were generated for an isosurface of electron density for individual molecules as well as for the vdW complexes using GaussView.⁵² The blue color denotes regions of strong positive potential and the red color denotes the regions of strong negative potential. The other colors, namely, green and yellow, represent intermediate values of electrostatic potential. The expected contrast between the electrostatic potential of benzene and hexafluorobenzene becomes clear in Figure 4. The former shows a red color in the middle of the ring, while the latter has a big spread of blue color in the middle of the ring and the red color is confined to the periphery because of the presence of the six F atoms. There is an alternation of red and blue in the periphery of 1,3,5-trifluorobenzene because of the presence of alternating F atoms.

Figure 5 illustrates the molecular electrostatic potential (MESP) maps for the different geometries of C₆H₆–X and C₆F₆–X (X = HF, H₂O, and NH₃) complexes. It is clear that when red (negative potential) and blue colors (positive potential) come within proximal limits, a stable complex is formed. On the other hand, when two figures of the same color (electrostatic potential of similar nature) approach, the result is an unstable complex. It was already shown in Figure 4 that the central

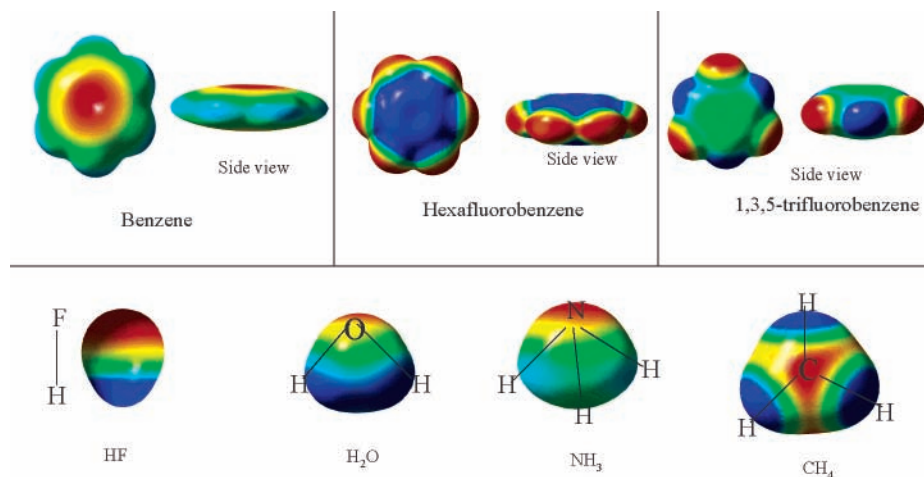


Figure 4. Molecular electrostatic potential isosurfaces for individual molecules. For the benzenoid systems, the top view and side view are shown. The blue color indicates large positive potentials, while the red color indicates large negative potentials. Green and yellow colors indicate intermediate values.

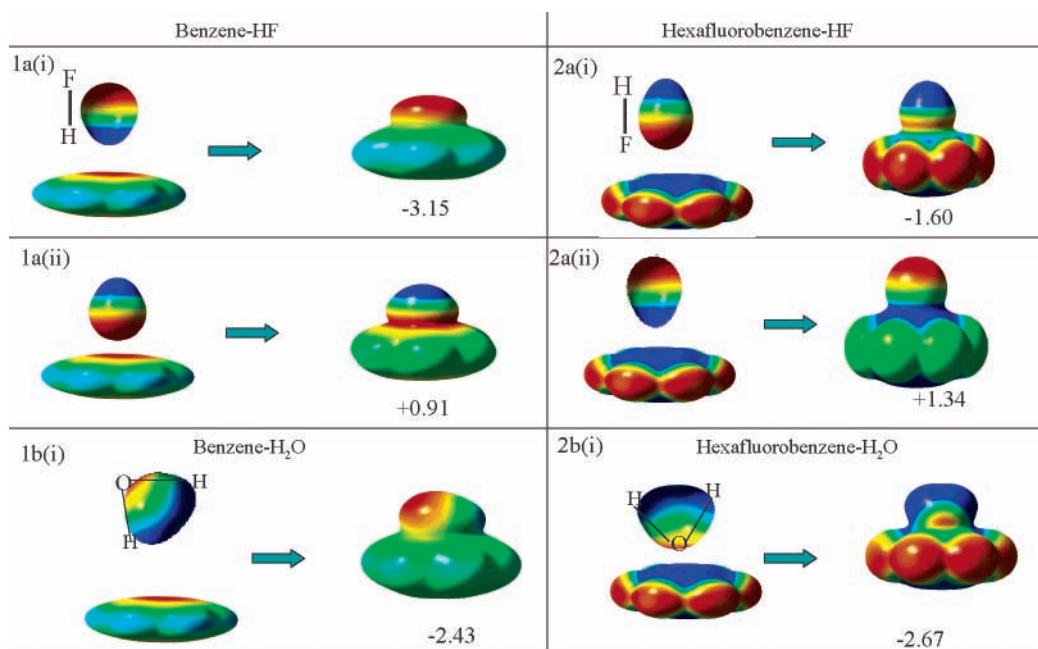


Figure 5. Same as in Figure 4 for different geometries of C_6H_6-X and C_6F_6-X , where $X = HF, H_2O,$ and NH_3 complexes.

portion of 1,3,5-trifluorobenzene shows a weak electrostatic potential. Therefore, the top-on geometries are expectedly not as stable as in the case of benzene/hexafluorobenzene complexes. Since the large positive and large negative potentials are confined to the periphery of 1,3,5-trifluorobenzene, the small molecules prefer to orient in such a way that they can form cyclic hydrogen bonds.

4. Summary and Conclusion

A detailed study of the geometry of vdW complexes of aromatic moieties with small molecules has yielded considerable insight into the intermolecular interaction. In the case of C_6H_6-X complex, the electropositive end of the molecule X points toward the benzene ring, which has a large negative quadrupole moment. The orientation gets reversed in C_6F_6-X because of the large positive quadrupole moment of C_6F_6 . Understandably, CH_4 , having neither a dipole moment nor a quadrupole moment, orients itself differently and forms a weakly bound complex. Since $C_6H_3F_3$ has nearly zero quadrupole

moment, the molecules $HF, H_2O, NH_3,$ and CH_4 prefer to lie in an end-on geometry forming hydrogen bonds.

Acknowledgment. This study was supported in part by a grant from the Council of Scientific and Industrial Research, New Delhi. We thank Dr. A. J. Stone for providing his software package, Orient 3.2 and Dr. Arunan (IISc Bangalore, India) for pointing out some of the earlier work on fluorobenzene systems. One of the authors (N.S.) thanks the Department of Science and Technology, New Delhi for a J. C. Bose fellowship.

Supporting Information Available: List of vibrational frequencies and graphics of the optimized geometries. This material is available free of charge via the Internet at <http://pubs.acs.org>.

References and Notes

- (1) Margenau, H. *Rev. Mod. Phys.* **1939**, *11*, 1.
- (2) Buckingham, A. D. *Adv. Chem. Phys.* **1967**, *12*, 107.
- (3) Stone, A. J. *The Theory of Intermolecular Forces*; Clarendon Press: Oxford, 1996.

- (4) Fowler, P. W.; Buckingham, A. D. *Can. J. Chem.* **1985**, *63*, 2018.
(5) Fowler, P. W.; Buckingham, A. D. *Chem. Phys. Lett.* **1991**, *176*, 11.
(6) Buckingham, A. D.; Fowler, P. W.; Hutson, J. M. *Chem. Rev.* **1988**, *88*, 963.
(7) Wormer, P. E. S.; Avoird, A. v. d. *Chem. Rev.* **2000**, *100*, 4109.
(8) Müller-Dethlefs, K.; Hobza, P. *Chem. Rev.* **2000**, *100*, 143.
(9) Meyer, E. A.; Castellano, R. K.; Deiderich, F. *Angew. Chem., Int. Ed.* **2003**, *42*, 1210.
(10) Suzuki, S.; Green, P. G.; Bumgarner, R. E.; Dasgupta, S.; Goddard, W. A., III; Blake, G. A. *Science* **1992**, *257*, 942.
(11) Gutowsky, H. S.; Emilsson, T.; Arunan, E. *J. Chem. Phys.* **1993**, *99*, 4883.
(12) Arunan, E.; Emilsson, T.; Gutowsky, H. S.; Fraser, G. T.; de Oliveira, G.; Dykstra, C. E. *J. Chem. Phys.* **2002**, *117*, 9766.
(13) Barth, H. D.; Buchhold, K.; Djafari, S.; Reimann, B.; Lommatzsch, U.; Brutschy, B. *Chem. Phys.* **1998**, *239*, 49.
(14) Gotch, A. J.; Zwier, T. S. *J. Chem. Phys.* **1992**, *96*, 3388.
(15) Augsperger, J. D.; Dykstra, C. E.; Zwier, T. S. *J. Phys. Chem.* **1993**, *97*, 980.
(16) Fredericks, S. Y.; Jordan, K. D.; Zwier, T. S. *J. Phys. Chem.* **1996**, *100*, 7810.
(17) Rodham, D. A.; Suzuki, S.; Suenram, R. D.; Lovas, F. J.; Dasgupta, S.; Goddard, W. A., III; Blake, G. A. *Nature* **1993**, *362*, 735.
(18) Kim, K. S.; Lee, J. Y.; Choi, H. S.; Kim, J.; Jang, J. H. *Chem. Phys. Lett.* **1997**, *265*, 497.
(19) Feller, D. *J. Phys. Chem. A* **1999**, *103*, 7558.
(20) Tarakeshwar, P.; Lee, S. J.; Lee, J. Y.; Kim, K. S. *J. Chem. Phys.* **1998**, *108*, 7217.
(21) Tsuzuki, S.; Honda, K.; Uchimaru, T.; Mikami, M.; Tanabe, K. *J. Am. Chem. Soc.* **2000**, *122*, 11450.
(22) Tsuzuki, S.; Honda, K.; Uchimaru, T.; Mikami, M.; Tanabe, K. *J. Phys. Chem. A* **2002**, *106*, 4423.
(23) Samanta, U.; Chakrabarti, P.; Chandrasekhar, J. *J. Phys. Chem. A* **1998**, *102*, 8964.
(24) Tsuzuki, S.; Honda, K.; Uchimaru, T.; Mikami, M.; Tanabe, K. *J. Am. Chem. Soc.* **2000**, *122*, 3746.
(25) Vrbancich, J.; Ritchie, G. L. D. *J. Chem. Soc., Faraday Trans. 2* **1980**, *76*, 648.
(26) Luhmer, M.; Bantik, K.; Dejaegere, A.; Bovy, P.; Reisse, J. *Bull. Chem. Soc. Fr.* **1994**, *131*, 603.
(27) Danten, Y.; Tassaing, T.; Besnard, M. *J. Phys. Chem. A* **1999**, *103*, 3530.
(28) Dunitz, J. D.; Taylor, R. *Chem. Eur. J.* **1997**, *3*, 89.
(29) Alkorta, I.; Rozas, I.; Elguero, J. *J. Org. Chem.* **1997**, *62*, 4687.
(30) Alkorta, I.; Rozas, I.; Elguero, J. *J. Am. Chem. Soc.* **2002**, *124*, 8593.
(31) Patrick, C. R.; Prosser, G. S. *Nature* **1960**, *187*, 1021.
(32) Williams, J. H.; Cockcroft, J. K.; Fitch, A. N. *Angew. Chem.* **1992**, *31*, 1655.
(33) Baiocchi, F. A.; Williams, J. H.; Klemperer, W. *J. Phys. Chem.* **1983**, *87*, 2079.
(34) Tarakeshwar, P.; Kim, K. S.; Brutschy, B. *J. Chem. Phys.* **1999**, *110*, 8501.
(35) Sanz, M. E.; Antolínez, S.; Alonso, J. L.; López, J. C.; Kuczkowski, R. L.; Peebles, S. A.; Peebles, R. A.; Boman, F. C.; Kraka, E.; Cremer, D. *J. Chem. Phys.* **2003**, *118*, 9278.
(36) Williams, J. H. *Acc. Chem. Res.* **1993**, *26*, 593.
(37) Gallivan, J. P.; Dougherty, D. A. *Org. Lett.* **1999**, *1*, 103.
(38) Raimondi, M.; Calderoni, G.; Famulari, A.; Raimondi, L.; Cozzi, F. *J. Phys. Chem. A* **2003**, *107*, 772.
(39) Tsuzuki, S.; Honda, K.; Uchimaru, T.; Mikami, M.; Tanabe, K. *J. Am. Chem. Soc.* **2002**, *124*, 104.
(40) Sinnokrot, M.; Sherrill, C. D. *J. Am. Chem. Soc.* **2004**, *126*, 7690.
(41) Mishra, B. K.; Sathyamurthy, N. *J. Phys. Chem. A* **2005**, *109*, 6.
(42) Mishra, B. K.; Sathyamurthy, N. *J. Theor. Comput. Chem.* **2006**, *5*, 609.
(43) *Gaussian 03*, Revision B.05. Frisch, M. J.; Trucks, G. W.; Schlegel, H. B.; Scuseria, G. E.; Robb, M. A.; Cheeseman, J. R.; Montgomery, Jr., J. A.; Vreven, T.; Kudin, K. N.; Burant, J. C.; Millam, J. M.; Iyengar, S. S.; Tomasi, J.; Barone, V.; Mennucci, B.; Cossi, M.; Scalmani, G.; Rega, N.; Petersson, G. A.; Nakatsuji, H.; Hada, M.; Ehara, M.; Toyota, K.; Fukuda, R.; Hasegawa, J.; Ishida, M.; Nakajima, T.; Honda, Y.; Kitao, O.; Nakai, H.; Klene, M.; Li, X.; Knox, J. E.; Hratchian, H. P.; Cross, J. B.; Bakken, V.; Adamo, C.; Jaramillo, J.; Gomperts, R.; Stratmann, R. E.; Yazyev, O.; Austin, A. J.; Cammi, R.; Pomelli, C.; Ochterski, J. W.; Ayala, P. Y.; Morokuma, K.; Voth, G. A.; Salvador, P.; Dannenberg, J. J.; Zakrzewski, V. G.; Dapprich, S.; Daniels, A. D.; Strain, M. C.; Farkas, O.; Malick, D. K.; Rabuck, A. D.; Raghavachari, K.; Foresman, J. B.; Ortiz, J. V.; Cui, Q.; Baboul, A. G.; Clifford, S.; Cioslowski, J.; Stefanov, B. B.; Liu, G.; Liashenko, A.; Piskorz, P.; Komaromi, I.; Martin, R. L.; Fox, D. J.; Keith, T.; Al-Laham, M. A.; Peng, C. Y.; Nanayakkara, A.; Challacombe, M.; Gill, P. M. W.; Johnson, B.; Chen, W.; Wong, M. W.; Gonzalez, C.; and Pople, J. A. *Gaussian, Inc.*: Wallingford, CT, 2003.
(44) Boys, S. F.; Bernardi, F. *Mol. Phys.* **1970**, *19*, 553.
(45) Amos, R. D. *CADPAC: The Cambridge Analytical Derivatives Package*; Issue 6, Technology report; University of Cambridge: Cambridge, U.K., 1995; A suite of quantum chemistry programs developed by Amos, R. D. with contributions from Alberts, I. L. et al.
(46) Stone, A. J.; Dullweber, A.; Hodges, M. P.; Popelier, P. L. A.; Wales, D. J. *Orient, a program for studying interactions between molecules*, version 3.2; University of Cambridge: Cambridge, U.K., 1995.
(47) Weast, R. C. *Handbook of Chemistry and Physics*; The Chemical Rubber Co.: Cleveland, OH, 1967.
(48) Brédas, J. L.; Street, G. B. *J. Am. Chem. Soc.* **1988**, *110*, 7001.
(49) Gadre, S. R.; Shirsat, R. N. *Electrostatics of Atoms and molecules*; Universities Press: Hyderabad, India, 2000.
(50) Gadre, S. R.; Deshmukh, M. M.; Chakraborty, T. *Chem. Phys. Lett.* **2004**, *384*, 350.
(51) Gadre, S. R.; Deshmukh, M. M.; Kalagi, R. P. *Proc. Indian Natl. Sci. Acad.* **2004**, *70A*, 709.
(52) Dennington, R., II; Keith, T.; Millam, J.; Eppinnett, K.; Hovell, W. L.; Gilliland, R. *GaussView*, Version 3.09; Semichem, Inc.: Shawnee Mission, KS, 2003.